SAINS TANAH – Journal of Soil Science and Agroclimatology, 23(2), 2026, 142-156

SAINS TANAH – Journal of Soil Science and Agroclimatology

Journal homepage: http://jurnal.uns.ac.id/tanah

Influence of charged-biochar and arbuscular mycorrhizal fungi on rice cell wall composition in iron toxicity-prone soils

Jamilah[1], Maradona[1], Fridarti[2], Yulfi Desi[3], Nur Qursyna Boll Kasim[4], Inawaty Sidabalok[5], Chrisnawati[6]

[1] Department of Agrotechnology, Faculty of Agriculture, Tamansiswa University, West Sumatra, 25138, Indonesia
[2] Department of Animal Husbandry, Agriculture Faculty, Tamansiswa University, 25139, Indonesia
[3] Department of Agrotechnology, Faculty of Agriculture, Universitas Ekasakti, West Sumatera, Indonesia
[4] Soil Conservation and Management Research Initiative Group (RIG), Faculty of Plantation and Agrotechnology, Universiti Teknologi MARA, Jasin Campus, Merlimau, Melaka, 77300, Malaysia
[5] Department of Agricultural Product Technology, Faculty of Agriculture, Ekasakti University, West Sumatera, Indonesia
[6] Department of Agrotechnology, Faculty of Agriculture. Universitas Mahaputra Muhammad Yamin, Solok, West Sumatera, 23171, Indonesia

ARTICLE INFO

Keywords:
Acidic paddy soils
Lignin biosynthesis
Soil–plant relationships
Biomass enhancement
Cell wall modification

Article history
Submitted: 2025-10-26
Revised: 2026-01-08
Accepted: 2026-03-16
Available online: 2026-09-05
Published regularly: December 2026

Corresponding Author
Email address:
** jamilah@unitas-pdg.ac.id*

ABSTRACT

Iron toxicity severely constrains rice production on acidic soils by inducing nutrient imbalance and suppressing biomass accumulation. This study evaluated the effects of charged biochar and arbuscular mycorrhizal fungi (AMF) on rice growth, nutrient status, and cell wall dynamics under Fe-toxic conditions. A factorial experiment was conducted on a strongly acidic Ultisols (pH 4.63; Fe 3616.89 ppm) with AMF inoculation (0, 5, and 10%) and charged-biochar application (0, 2.5, and 5 t ha^{-1}). Both amendments significantly improved plant height, shoot dry weight, and forage dry weight (FDW), primarily through enhanced vegetative growth, nutrient-use efficiency, and root development. AMF colonization reached 68%, while charged biochar effectively ameliorated soil acidity and Fe stress. Regression analysis identified shoot dry weight, nitrogen content, ash (silica) content, and AMF colonization as the main determinants of FDW (R^2 = 0.996), whereas excessive plant phosphorus negatively affected yield. Cell wall components showed no direct association with FDW but contributed to tissue structural integrity. The combined application of charged biochar and AMF, supported by improved silica accumulation, provides an effective strategy to mitigate Fe toxicity and enhance rice forage productivity on acidic soils.

How to Cite: Jamilah, Maradona, Fridarti, Desi, Y., Kasim, N. Q. B., Sidabalok, I., & Chrisnawati. (2026). Influence of charged-biochar and arbuscular mycorrhizal fungi on rice cell wall composition in iron toxicity-prone soils. Sains Tanah Journal of Soil Science and Agroclimatology, 23(2), 142-156. https://doi.org/10.20961/stjssa.v23i2.110381

1. INTRODUCTION

Rice is the staple food crop for many nations worldwide. However, paddy fields are not always established on fertile soils; many are acidic, low in nutrient availability, high in soluble iron (Fe), and poor in organic matter. The Fe concentration in soil that triggers toxicity symptoms varies considerably depending on environmental conditions and plant species. Studies have shown that, in rice, Fe toxicity symptoms appear at specific Fe concentrations in soil solution, particularly under flooded conditions. Severe toxicity symptoms are observed at Fe concentrations ≥ 325 ppm (Noor et al., 2012). In certain soils, such as Ultisols, Fe levels can reach as high as 4881 ppm, posing a significant risk of Fe toxicity to rice production (Ahmed et al., 2023). Similarly, the experimental soil used in this study contained Fe concentrations as high as 3616.89 ppm.

The rice cell wall is composed of structural fiber fractions—hemicellulose, cellulose, and lignin—together with inorganic mineral components such as silica (SiO_2). The relationships (Ramírez-Olvera et al., 2021) among silica, lignin, hemicellulose, and cellulose contents in rice plants significantly influence growth and structural integrity. Silica accumulation affects the balance of carbon-based compounds, including cellulose and lignin, which are critical for plant health and ecosystem functioning. Silica does not directly improve the quality of cellulose and lignin; rather, it may operate through substitution or metabolic trade-off mechanisms, reducing carbon energy requirements and enabling plants to conserve carbon for growth through a carbon-sparing strategy. The interactions among these components can either enhance or limit plant growth,

STJSSA, p-ISSN 1412-3606 e-ISSN 2356-1424
http://dx.doi.org/10.20961/stjssa.v23i2.110381
© 2026 The Authors. Published by Universitas Sebelas Maret
This is an open-access article under the CC BY NC license (http://creativecommons.org/licenses/by/4.0/)

depending on their concentrations and relative proportions. Rice is known for its exceptional ability to accumulate silica, which can constitute up to 10% of shoot dry weight (Du et al., 2022). Silicon enhances both shoot and root biomass, thereby promoting overall plant growth (Mundada et al., 2021; Ramírez-Olvera et al., 2021). There is no strong evidence that silica reduces essential carbon compounds; on the contrary, many studies demonstrate that silica can conserve carbon and reinforce cell walls, thereby supporting plant health and resilience (Schaller et al., 2019).

Several studies suggest that lignin accumulation may increase under high-silica conditions, not only during silicon deficiency. The findings of Mir et al. (2022) are therefore valid but should not be generalized as a universal physiological mechanism across all plant species. Similarly, cellulose deposition is often elevated in the absence of silicon, indicating that silicon plays a regulatory role in cell wall composition (Ghouri et al., 2022). Maintaining a balance between lignin and cellulose is thus essential for preserving structural integrity and resistance to environmental stress. Hemicellulose, together with cellulose and lignin, contributes to the overall structural framework of rice plants. The composition of rice husk, which contains approximately 18–21% hemicellulose, further highlights its potential for diverse applications such as biofuel production and soil amendment (Mishra et al., 2023; Nawaz et al., 2023). While silica accumulation and its interactions with lignin and cellulose generally promote rice growth, excessive silica may reduce the availability of essential carbon compounds, thereby influencing plant and ecosystem performance.

The application of biochar, particularly rice husk biochar (RHB), has been shown to significantly increase silica levels in rice plants (de Tombeur et al., 2021). Numerous studies have demonstrated that biochar not only enhances silicon availability in soil but also promotes leaf silicification, thereby improving plant resilience and yield (Guo et al., 2020; Hailegnaw et al., 2019). Rice husk biochar serves as a readily available source of plant-available silicon; Olanrewaju et al. (2024) reported that its application increased pore-water silicon concentrations by up to 39.5% during the reproductive stage of rice growth. Research conducted between 2020 and 2024 has increasingly clarified carbon allocation patterns and the mechanical functions of silica, lignin, and cellulose through metabolomics and cell-wall modelling approaches (e.g. Yao et al. (2022)). The use of rice-derived biochar can increase leaf silicon concentrations from 19.0 to 70.4 g kg^{-1}, leading to greater silica deposition in rice leaves (Jabborova et al., 2022). Biochar application has also been associated with improved leaf characteristics, although some studies have reported reductions in leaf mass per area (LMA), suggesting complex interactions between biochar treatments and plant physiological responses (Pouangam Ngalani et al., 2023; Wen et al., 2022). Under normal conditions, LMA increases with silica and biochar application due to cell wall thickening; where LMA decreases, contextual factors such as excessive biochar dosage, nutrient immobilization, nitrogen deficiency, or physiological stress must be considered. The effectiveness of biochar can therefore vary depending on the method and rate of application, with some instances reporting yield reductions linked to nutrient immobilization (Olanrewaju et al., 2024; Shifa et al., 2025).

Sustainable fertilization and soil amelioration technologies are thus essential to enhance rice performance while simultaneously supplying high-quality forage (Aufa Ain & Noraini, 2023). Two promising approaches are arbuscular mycorrhizal fungi (AMF) and charged biochar. AMF enhances nutrient uptake, particularly phosphorus (P), by extending root exploration zones and secreting phosphatases that mobilize insoluble P (Huang et al., 2021; Khaliq et al., 2022). Biochar, in contrast, functions as a soil amendment that improves pH, cation exchange capacity, soil structure, and microbial habitat, thereby supporting nutrient retention and microbial diversity (Akbar et al., 2023; Mulyadi & Jiang, 2023). Synergistic interactions between AMF and biochar have been shown to significantly enhance P uptake and plant biomass, particularly in P-deficient soils (Alotaibi et al., 2023; Meng et al., 2024; Sun et al., 2022).

Charged biochar, defined as biochar enriched with Crocober Plus liquid organic fertilizer (LOF) and phosphate-solubilizing bacteria (PSB), has the potential to further improve nutrient delivery and AMF colonization. Crocober Plus supplies nitrogen, phosphorus, potassium, humic and alginic acids, and amino acids, while stimulating microbial activity and plant growth, with reported increases in rice yield of up to 6.34 t ha^{-1} of dry grain (Jamilah et al., 2021). Previous studies have also demonstrated that AMF–biochar co-application can enhance P uptake by up to 67%, improve soil microbial communities, and mitigate greenhouse gas emissions in paddy systems (Meng et al., 2024; Saikanth et al., 2023; Wen et al., 2024).

Despite these promising findings, research on the interaction between AMF and charged biochar under flooded acidic paddy soils remains limited, particularly with respect to forage productivity as a value-added by-product of rice cultivation. This study therefore aimed to elucidate the mechanistic relationships linking AMF–charged biochar interactions, plant physiological traits, cell wall composition, and forage dry weight (FDW) in flooded acidic paddy soils.

2. MATERIALS AND METHODS

2.1. Study Site and Experimental Design

The study was conducted in Nagari Tigo Koto Silungkang, Palembayan Sub-district, Agam Regency, West Sumatera, Indonesia, located at 00°09′22″ S and 100°08′17″ E, at an altitude of 498 m above sea level (Fig. 1). The soil is classified as Ultisol, a typical acidic paddy soil, which was puddled and prepared prior to transplanting. The study soil was classified as an Ultisols based on its strongly acidic reaction (pH H_2O 4.63), low cation exchange capacity (10.64 cmol kg^{-1}), very low exchangeable base contents, and low base saturation (24.31%), which is below the 35% threshold defined in USDA Soil Taxonomy. In addition, the very low available phosphorus (P) and high iron (Fe) content indicate advanced weathering and intensive leaching, which are characteristic of Ultisols in humid tropical environments. Complete soil analysis included pH (H_2O and KCl), nutrient content (N), C/N ratio, exchangeable base and acid cations, cation exchange capacity (CEC), and micronutrients such as Cu, Zn, Mn, and Fe. These analyses were conducted at the Laboratory of the West Sumatra Centre for the Implementation of Agricultural Instrument Standards (BPSIP), Indonesia. The soil laboratory is accredited in accordance with ISO/IEC 17025:2017 (Table 1).

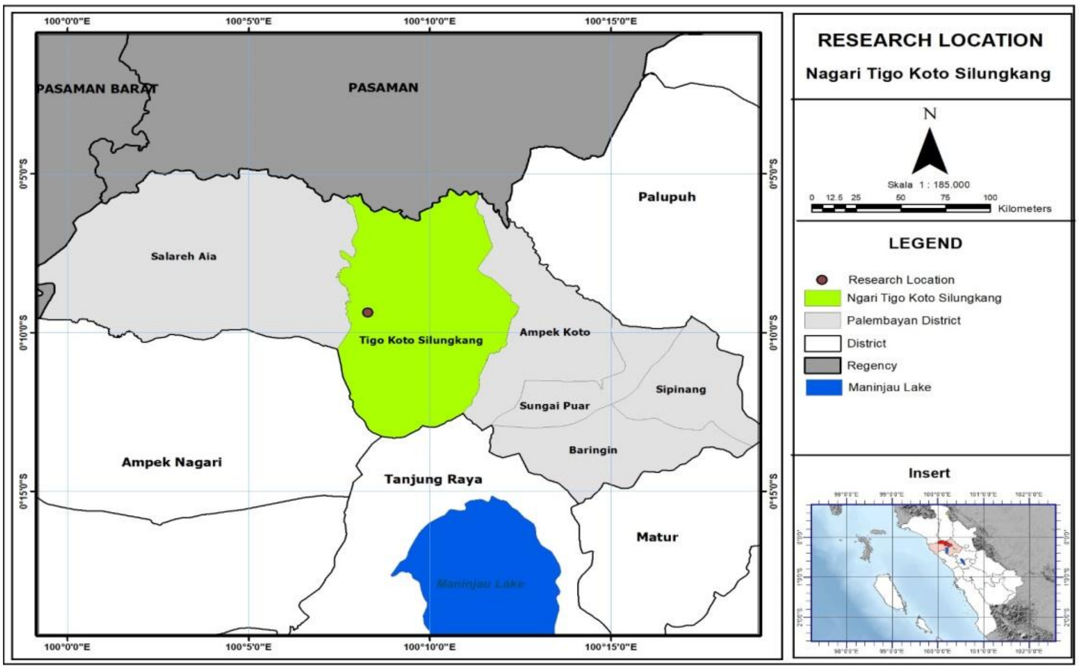

Figure 1. Study site at Nagari Tigo Koto Silungkang, Palembayan, Agam Regency

Table 1. Initial soil and charged-biochar chemical properties*

Property*)	Value	Criteria**)	range
pH H_2O (1:5)	4.63	acidic	4.5-5.5
pH KCl (1:5)	3.67		
Organic-C (%)	2.72	moderate	2-3
N (%)	0.3	moderate	0.21-0.5
C/N	9.07	low	
P_2O_5 Bray-1 (ppm)	7.28	Very low	<15
Exchangeable bases (cmol kg^{-1})			
Exchangeable K	0.09	Very low	<0.1
Exchangeable Ca	0.034	Very low	<2
Exchangeable Mg	0.002	Very low	<0.3
Exchangeable Na	0.25	low	<0.1
Total bases	0.38	-	
Base saturation (%)	24.31	low	20-40
exchangeable acidity (cmol kg^{-1})			
Exchangeable Al	0.81	-	
Exchangeable H	0.36	-	
Total acidity (cmol kg^{-1})	1.17	-	
Al saturation (%)	7.61	low	>40
CEC (cmol kg^{-1})	10.64	low	5-16
Micro elements (ppm) H_2SO_4-$HClO_4$ extract			
Cu	0	deficiency	0.2
Zn	120.3	Very high	>1
Mn	163.71	Very high	23
Fe	3616.89	Very high	53
Charged-Biochar nutrients (%)			
Total-N	0.27	low	9.8
P_2O_5	0.68	low	10
K_2O	0.83	high	0.2
Ash	41.77		
Organic-C	33.84		

Remarks: *Analysed at the BPTP West Sumatra Laboratory, 2025; ***Criteria based on* Tripathi et al. (2018).

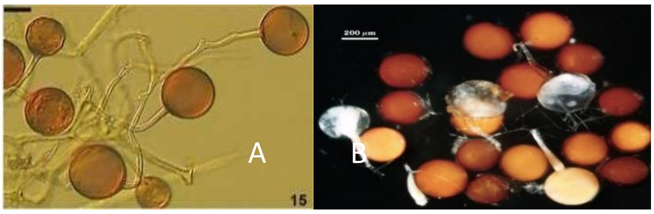

Figure 2. Glomus sp.(A) and Acaulospora sp.(B) (Courtesy of Magurno et al. (2024) and da Silva et al. (2022)).

2.2. Mycorrhizal Inoculum

A consortium of arbuscular mycorrhizal fungi (AMF), comprising *Glomus* sp. and *Acaulospora* sp., was used in this study (Fig. 2). The inoculum was mass-multiplied under greenhouse conditions using zeolite as a carrier medium and sorghum (*Sorghum bicolor* L.) as the host plant. Zeolite provided a porous and chemically stable matrix that supported spore survival and hyphal development, while sorghum facilitated rapid root colonization and AMF proliferation. After 10–12 weeks, the inoculum, consisting of zeolite particles, AMF spores, extraradical hyphae, and colonized root fragments, was harvested, air-dried, and homogenised. Inoculum quality was assessed based on spore density and viable propagule density. Spore density was determined using the wet sieving and decanting method and averaged approximately 125 spores per 5 g of inoculum. Viable propagule density, representing infective AMF units capable of initiating root colonization, was estimated using a host-plant bioassay and expressed as 1×10^5 CFU-equivalent g^{-1} inoculum.

2.3. Experimental Design and Treatments

The experiment was arranged in a factorial Randomised Block Design (RBD) with two factors: AMF inoculation in seedbed media at 0, 5, and 10% (v/v), and charged-biochar application at 0, 2.5, and 5 t ha^{-1}. Each treatment was replicated three times. Data were subjected to analysis of variance (ANOVA) at a 5% significance level, and mean separation was conducted using the least significant difference (LSD) test at a 5% probability level.

2.4. Statistical Analysis Using Pearson Correlation and Multiple Regression

Pearson's correlation analysis (bivariate) was performed to evaluate the strength and significance of relationships between measured variables using a two-tailed test at a significance level of $\alpha = 0.05$. Variables showing strong and significant correlations with forage dry weight (FDW) at 50 days after transplanting (DAT) were identified and interpreted based on the magnitude and direction of the correlation coefficients. A significant positive correlation indicated a supportive contribution to biomass accumulation, whereas a significant negative correlation indicated an inverse relationship; non-significant correlations were considered indicative of weak or no linear association. To further assess the combined influence of multiple factors on plant biomass, multiple linear regression analysis was conducted with FDW at 50 DAT as the dependent variable. The significance of individual predictor variables was evaluated using t-tests after accounting for the effects of other variables in the model. All statistical analyses were conducted using appropriate statistical software (e.g. SPSS or R), and statistical significance was declared at $p \leq 0.05$.

2.5. Charged-Biochar Preparation

Rice husk biochar was produced via pyrolysis under low-oxygen conditions to prevent complete combustion. The charging process involved mixing 1 tonne of fresh biochar with 10 L of phosphate-solubilizing bacteria (PSB; *Pseudomonas fluorescens* at 1.2×10^{13} CFU mL^{-1} and *Bacillus subtilis* at 1.6×10^{13} CFU mL^{-1}), 20 L of Crocober Plus liquid organic fertilizer (LOF), and 50 L of water, followed by incubation for 48 h.

2.6. Propagation of Phosphate-Solubilizing Bacteria (PSB) and Preparation of Charged Biochar

The propagation of phosphate-solubilizing bacteria (PSB) was conducted at the Laboratory of the Faculty of Agriculture, Universitas Tamansiswa Padang. PSB were isolated from paddy soil collected *in vivo* at a depth of 5–15 cm and subsequently propagated. A soil suspension was prepared by dissolving 10 g of soil in physiological NaCl solution (0.85%) and shaking the mixture for 30 minutes to detach microorganisms from soil particles. Serial dilutions were then carried out up to 10^{-6}, and 0.1 mL from each dilution was inoculated onto Pikovskaya agar (PVK) medium and incubated at 28–30°C for 3–5 days.

Selection of PSB colonies was based on the formation of clear halos around colonies, indicating phosphate solubilization. Selected colonies were purified through repeated subculturing. Laboratory-scale propagation of PSB cultures was performed using Pikovskaya liquid medium prepared in 500 mL Erlenmeyer flasks and sterilised by autoclaving at 121°C for 15 minutes. Inoculation was carried out by transferring one loopful of PSB culture into the sterile liquid medium, followed by incubation on a shaker at 150 rpm for 3–5 days at 30°C. Harvesting was conducted after optimal growth was achieved, with a recommended cell density of 10^7–10^9 CFU mL^{-1}, which was verified using the Total Plate Count (TPC) method prior to application.

Charged biochar was prepared using a ratio of 1 tonne of biochar combined with 10 L of PSB suspension (10^{13} CFU mL^{-1}) and 20 L of Crocober Plus liquid organic fertilizer (POC). The preparation of Crocober Plus followed established guidelines (Jamilah et al., 2021). The PSB suspension and POC were diluted in 50 L of water, after which 1 tonne of biochar was immersed in the solution for 48 h to allow optimal absorption of microorganisms and nutrients. Subsequently, following the procedure described by Selvarajh et al. (2024), the biochar was drained and air-dried to approximately 50% moisture content prior to field application. The charged biochar was applied at the beginning of planting according to the respective treatment doses.

2.7. Parameters Measured

The following parameters were measured. Soil properties: Soil pH (H_2O, 1:5). Plant growth: Plant height, tiller number, leaf area index (LAI), net assimilation rate (NAR), and relative growth rate (RGR) at 50 days after transplanting (DAT). AMF colonisation: Root infection percentage was determined using the root clearing and staining technique. Root samples were carefully washed with distilled water to remove adhering soil and cut into 1 cm segments. From each sample, ten root segments were randomly selected and placed on a clean microscope slide.

The root segments were cleared in 10% (w/v) KOH at 90°C for 30–60 min, rinsed thoroughly with distilled water, and acidified in 1% HCl for 10–15 min. Roots were then stained with 0.05% trypan blue in lactoglycerol (or aniline blue as an alternative) at 90°C for 15–30 min, followed by destaining in lactoglycerol to remove excess stain. The stained root segments were mounted on microscope slides and observed under a compound microscope (×100–×400). Each root segment was examined for the presence of AMF structures, including hyphae, arbuscules, and vesicles. Root infection percentage was calculated using Formula 1.

$$\text{AMF colonization } (\%) = \frac{\text{Number of root segments showing AMF structures}}{\text{Total number of observed root segments } (10)} \times 100 \quad [1]$$

Forage quality: Ash content and forage yield at 50 DAT, cellulose, hemicellulose, lignin, silica. The chemical composition of the rice plant tissues, including cellulose, hemicellulose, lignin, and silica, was analysed using standard methods (Kostryukov et al., 2023). Cellulose content was determined using the acid detergent fibre (ADF) method, in which plant material was treated with acid detergent to remove hemicellulose and soluble compounds, leaving cellulose as the primary residue, which was then quantified gravimetrically. Hemicellulose content was estimated indirectly as the difference between neutral detergent fibre (NDF) and ADF fractions, where NDF represents cellulose, hemicellulose, and lignin, and ADF represents cellulose and lignin. In addition, acid hydrolysis followed by sugar analysis can be used to quantify hemicellulose-derived sugars when higher precision is required. Lignin was determined using the acid detergent lignin (ADL) method, where the residue obtained from the ADF treatment was further treated with concentrated sulfuric acid to remove cellulose, leaving lignin, which was then washed, dried, and weighed**.** Silica (SiO_2) content was measured by ashing the plant material at high temperature (500–600°C) and dissolving the ash in acid, followed by either gravimetric determination of insoluble silica or colorimetric analysis using the molybdenum blue method. All analyses were conducted in triplicate to ensure accuracy and reproducibility.

Protein yield was determined using crude protein analysis by the Kjeldahl method**.** Dried and ground plant samples were analysed for total nitrogen, and crude protein concentration was calculated as N × 6.25. Protein yield (kg ha^{-1}) was obtained by multiplying crude protein concentration by shoot dry matter yield per hectare.

Growth Indices Calculation, Leaf Area Index (LAI) (Ribeiro et al., 2019), in Formula 2.

$$LAI = \frac{\text{Total leaf area per hill } (cm^2)}{\text{Ground area occupied by the hill } (cm^2)} \quad [2]$$

$$\text{Leaf area } (cm^2) = \text{Leaf length (cm)} \times \text{Maximum width (cm)} \times k$$


Figure 3. Leaf bronzing symptoms on older rice leaves under treatment C_0B_0 (1) and the absence of symptoms under treatment C_2B_2 (2) at 65 DAT.

where *k* = correction factor for rice leaf shape (0.75).

Net Assimilation Rate (NAR), at Formula 3**.**

$$NAR = \frac{W2-W1}{t2-t1} \times \frac{\ln A2-\ln A1}{A2-A1} \quad [3]$$

where W_1, W_2 = plant dry weight at times t_1, t_2; A_1, A_2 = total leaf area; ln = natural logarithm.

Relative Growth Rate (RGR) at Formula 4.

$$LPR = \frac{\ln W2-\ln W1}{t2-t1} \quad [4]$$

Ash content (%) (gravimetric method) in Formula 5.

$$\text{Ash } (\%) = \frac{Wdry-Wash}{Wdry} \times 100 \quad [5]$$

where *Wdry* = oven-dried weight at 105°C until constant weight; *Wash* = residue weight after ignition at 500°C for 5 h in a muffle furnace.

The assessment of iron toxicity symptoms in rice plants was conducted exclusively based on visual symptom expression using standardized reference images developed by the International Rice Research Institute (IRRI). Visual scores were used solely for descriptive purposes and were not subjected to statistical analysis.

3. RESULTS

3.1. Rhizosphere Soil Chemistry

The initial soil analysis (Table 1) showed strongly acidic conditions with high exchangeable Al and soluble Fe, both of which are limiting factors for rice in acidic soils. Excess Zn and Mn also indicated risks of nutrient imbalance and toxicity. Under prolonged flooding, Fe toxicity appeared at 65 DAT, marked by reddish-brown bronzing on older leaves (Fig. 3). This coincided with very high soil Fe (3616.89 ppm), as flooding accelerates the reduction of Fe^{3+} to soluble Fe^{2+}.

3.2. Root Infection by AMF and Charged Biochar on Plant Dry Weight and LAI at 30 DAT, Root Dry Weight, AMF Infection and P-concentration at 50 DAT

Based on the ANOVA results, AMF, charged biochar, and their interaction had significant effects on root dry weight and AMF root colonization at 50 DAT ($p < 0.05$). In contrast, biochar alone did not have a significant effect on root length (Table 2). At 30 DAT, significant effects of AMF, charged biochar, and their interaction were also observed on plant dry weight and leaf area index (LAI) ($p < 0.05$).

Table 2. Interaction of AMF and charged-biochar on plant dry weight and LAI at 30 DAT, root dry weight, AMF colonization and plant P concentration at 50 DAT

Application of AMF and charged biochar	At 30 DAT		At 50 DAT		
	Plant dry weight per clump (g)	LAI	Weight of dry root (g)	AMF infection in root (%)	Plant P concentration (%)
C_0B_0	2.01 ± 0.48^c	1.14 ± 0.13^d	21.20 ± 2.83^c	50.00 ± 0.00^{bc}	0.087±0.009^c
C_0B_1	3.24 ± 0.17^b	1.35 ± 0.34^{cd}	20.49 ± 2.91^c	86.67 ± 8.89^a	0.113±0.011^{bc}
C_0B_2	2.81 ± 0.32^{bc}	1.40 ± 0.08^c	20.91 ± 3.34^c	60.00 ± 6.67^b	0.140±0.007^a
C_1B_0	2.64 ± 0.22^c	1.26 ± 0.23^d	14.25 ± 1.85^d	86.67 ± 4.44^a	0.117±0.004^b
C_1B_1	3.13 ± 0.32^b	1.81 ± 0.32^b	17.96 ±3.47^{cd}	56.67 ± 8.89^{bc}	0.117±0.004^b
C_1B_2	4.83 ± 0.21^a	1.80 ± 0.09^b	33.73 ± 1.29^b	60.00 ± 6.67^b	0.093±0.016^c
C_2B_0	3.63 ± 0.35^{ab}	1.67 ± 0.10^{bc}	29.49 ± 4.14^b	36.67± 5.44^c	0.120±0.013^{ab}
C_2B_1	3.17 ± 0.26^{bc}	1.61 ± 0.17^{bc}	43.96 ± 4.14^a	63.33 ± 4.44^b	0.113±0.009^{bc}
C_2B_2	4.62 ± 0.51^a	2.45 ± 0.00^a	37.20 ±2.96^{ab}	80.00 ± 6.67^a	0.107±0.004^{bc}
CV (%)	14.07	13.80	14.74	13.81	11.72

Notes: Mean values in each column marked with different letters indicate statistically significant differences among treatments for AMF or biochar, based on LSD Test at the 5% significance level ($p < 0.05$). Data are presented as mean ± standard deviation. CV = Coefficient of Variation.

Description: C_0B_0 = 0% AMF in the seedbed medium + 0 tons ha^{-1} charged biochar; C_0B_1 = 0% AMF in the seedbed medium + 2.5 tons ha^{-1} charged biochar; C_0B_2 = 0% AMF in the seedbed medium + 5.0 tons ha^{-1} charged biochar; C_1B_0 = 5% AMF in the seedbed medium + 0 tons ha^{-1} charged biochar; C_1B_1 = 5% AMF in the seedbed medium + 2.5 tons ha^{-1} charged biochar; C1B2 = 5% AMF in the seedbed medium + 5.0 tons ha^{-1} charged biochar; C_2B_0 = 10% AMF in the seedbed medium + 0 tons ha^{-1} charged biochar; C_2B_1 = 10% AMF in the seedbed medium + 2.5 tons ha^{-1} charged biochar; C_2B_2 = 10% AMF in the seedbed medium + 5.0 tons ha^{-1} charged biochar.

Numerical results showed that, at 30 DAT, plant dry weight and LAI were higher in treatments receiving AMF and charged biochar than in the control (C0B0). The highest plant dry weight (4.83 g) was recorded in treatment C1B2 (5% AMF + 5 t ha^{-1} charged biochar), whereas the maximum LAI (2.45) was observed in C2B2 (10% AMF + 5 t ha^{-1} charged biochar).

At 50 DAT, root dry weight varied significantly among treatments. The highest root dry weight (43.96 g) was obtained in treatment C2B1 (10% AMF + 2.5 t ha^{-1} charged biochar). AMF root colonization ranged from 36.7% to 86.7%, with the highest colonization values recorded in treatments without biochar. Nevertheless, combined treatments such as C2B2 maintained relatively high AMF colonization (80%). Detailed mean comparisons for all parameters are presented in Table 2.

Based on the ANOVA results, plant P concentration was significantly affected by biochar application ($p < 0.05$), whereas the main effect of AMF and the AMF × biochar interaction were not significant (Table 2). Among the treatments, the highest plant P concentration was recorded in C0B2, corresponding to the highest biochar application rate without AMF. Treatments receiving AMF without biochar (C2B0) also showed a higher plant P concentration than the control, although values were lower than those observed in C0B2.

Across biochar levels, plant P concentration increased with increasing biochar dose irrespective of AMF inoculation. In combined treatments, plant P concentration did not exceed the values obtained under the highest biochar treatment alone. Mean values and statistical comparisons of plant P concentration across treatments are presented in Table 2.

3.3. Response of Rice Growth Components (Plant Height, Tiller Number, and Ash Content) to AMF and Charged Biochar during 30–50 DAT

ANOVA revealed significant effects of AMF inoculation and charged biochar application on rice growth traits between 30 and 50 DAT (Table 3). Plant height increased under both AMF inoculation and biochar application. At 30 DAT, the tallest plants were observed with 10% AMF (36.44 cm), while by 50 DAT, plant height reached 65.87 cm under 5 t ha^{-1} biochar. This improvement was associated with the combined application of AMF and charged biochar treatments. ANOVA showed that, at 30 DAT, tiller number was significantly affected by the main effects of AMF and charged biochar without a significant interaction, whereas at 50 DAT, only AMF had a significant main effect. Plant ash content was significantly affected only at 50 DAT; in general, higher doses of AMF and charged biochar increased ash concentration.

3.4. Responses of Rice Physiological Traits and Tissue Nutrient Content (NAR, RGR, LAI, Cellulose, and Hemicellulose) to AMF and Charged Biochar during the 30–50 DAT Period

The ANOVA results showed that AMF and charged biochar treatments had significant effects ($p < 0.05$) on several physiological traits of rice grown in acidic soils. While the net assimilation rate (NAR) remained relatively stable across treatments, both the relative growth rate (RGR) and leaf area index (LAI) responded positively. Cellulose and hemicellulose contents were not significantly affected by either AMF or biochar treatments. The highest RGR (79.65 mg g^{-1} day^{-1}) and LAI (3.52) were achieved with 10% AMF, while 5 t ha^{-1} charged biochar also supported greater canopy development (LAI 3.51) (Table 4). ANOVA results further demonstrated that AMF and charged biochar treatments significantly affected growth parameters, nutrient-associated traits, and forage productivity under acidic soil conditions.

Table 3. Effect of AMF and charged-biochar on plant height, number of tillers and ash content during 30-50 DAT period

Treatment	Plant height (cm)		Number of tillers		Ash-content (%)	
	30 DAT	50 DAT	30 DAT	50 DAT	30 DAT	50 DAT
AMF application in seedling media (%)						
0.0	32.83± 1.89^{b}	58.60±2.67^{a}	18.50±0.18^{b}	24.14±0.98^{b}	15.44±0.74a	11.44±1.16^{a}
5.0	35.89±1.63^{ab}	63.46±4.52^{a}	20.61±0.75^{ab}	25.44±1.41^{ab}	14.45±1.53^{a}	10.73±0.97^{a}
10.0	36.44±0.41^{a}	63.16±3.89^{a}	22.28±0.72^{a}	29.67±0.67^{a}	15.98±0.42^{a}	10.30±0.19^{a}
Charged- biochar (tons ha^{-1})						
0	34.44 ± 0.93^{a}	60.19±3.73^{ab}	19.33±1.00^{b}	27.03±1.76^{a}	14.92±1.84^{a}	10.22±0.08^{b}
2.5	33.94 ± 2.63^{a}	59.16±1.66^{b}	20.50±0.56^{ab}	24.89±2.52^{a}	15.38±0.10^{a}	10.27±0.41^{ab}
5.0	36.78 ± 1.18^{a}	65.87±3.83^{a}	21.56±0.76^{a}	27.33±2.22^{a}	15.60±0.69^{a}	11.99±0.93^{a}
CV (%)	7.22	8.42	7.54	14.95	15.52	13.86

Notes: Mean values in each column marked with different letters indicate statistically significant differences among treatments for AMF or biochar, based on LSD Test at the 5% significance level ($p < 0.05$). Data are presented as mean ± standard deviation. CV = Coefficient of Variation.

Table 4. Effect of AMF and charged biochar on NAR, RGR, LAI, cellulose, and hemicellulose during the 30–50 DAT period

Treatment	NAR (g m^{2} day^{-1})	RGR mg g^{-1} day^{-1}	LAI		Cellulose (%)	Hemicellulose (%)
	30-50 DAT		30 DAT	50 DAT		
AMF application in seedling media (%)						
0.0	4.14±0.21^{a}	78.11±1.40^{a}	1.29±0.104^{b}	2.35±0.39^{b}	29.42±0.65^{a}	29.18±1.58^{a}
5.0	3.81±0.14^{a}	71.71±2.47^{a}	1.62±0.24^{ab}	3.02±0.34^{ab}	28.57±1.09^{a}	28.81±0.96^{a}
10.0	4.00±0.39^{a}	77.13±6.61^{a}	1.91±0.36^{a}	3.52±0.46^{a}	29.25±0.53^{a}	31.87±1.95^{a}
Charged- biochar (tons ha^{-1})						
0.0	3.91±0.11^{a}	74.08±1.28^{a}	1.62±0.24^{ab}	2.75±0.48^{b}	29.02±1.06^{a}	30.69±2.53^{a}
2.5	4.24±0.39^{a}	79.65±4.93^{a}	1.91±0.36^{a}	2.62±0.45^{b}	29.11±0.73^{a}	30.91±1.27^{a}
5.0	3.79±0.20^{a}	73.22±4.34^{a}	1.29±0.104^{b}	3.51±0.46^{a}	29.12±0.69^{a}	28.26±0.59^{a}
CV (%)	14.43	10.86	15.55	18.61	8.89	15.67

Notes: Mean values in each column marked with different letters indicate statistically significant differences among treatments for AMF or biochar, based on LSD Test at the 5% significance level ($p < 0.05$). Data are presented as mean ± standard deviation. CV = Coefficient of Variation.

Table 5. Effect of AMF and charged biochar on mycorrhizal infection, root length, and root dry weight of rice plants during the 30–50 DAT period

Treatment	Michorrizhae Infection (%)		Root Length (cm)		Root Dry Weight (g hill^{-1})	
	30 DAT	50 DAT	30 DAT	50 DAT	30 DAT	50 DAT
AMF application in seedling media (%)						
0.0	25.56±10.37^{c}	65.55±14.07^{b}	17.81±0.41^{a}	23.69+1.09^{a}	2.42±0.13^{b}	20.87±0.25^{b}
5.0	48.89±10.37^{b}	67.78±12.59^{a}	18.33±1.07^{a}	26.08±0.99^{a}	4.27±1.08^{a}	21.98±7.83^{b}
10.0	62.22±12.59^{a}	60.00±15.56^{ab}	19.29±1.28^{a}	25.05±1.63^{a}	4.49±0.70^{a}	36.88±4.93^{a}
Charged- biochar (tons ha^{-1})						
0	57.78±16.29^{a}	57.78±19.26^{a}	19.03±0.53^{a}	23.52±0.76^{a}	3.85±0.71^{ab}	21.64±5.23^{b}
2.5	28.89±12.59^{b}	68.89±11.85^{a}	17.1±0.24^{a}	26.28±0.81^{a}	2.89±0.10^{b}	27.47±10.99^{ab}
5.0	50.00±11.11^{a}	66.67±8.88^{a}	19.3±0.96^{a}	25.02±1.69^{a}	4.41±0.63^{a}	30.61±6.47^{a}
CV (%)	15.30	14.39	15.34	11.57	15.01	14.74

Notes: Mean values in each column marked with different letters indicate statistically significant differences among treatments for AMF or biochar, based on LSD Test at the 5% significance level ($p < 0.05$). Data are presented as mean ± standard deviation. CV = Coefficient of Variation.

3.5. Responses of Mycorrhizal Infection, Root Traits, and Forage Yield Quality of Rice Plants to AMF and Charged Biochar during 30–50 DAT

The ANOVA results indicated that AMF inoculation had a significant effect on mycorrhizal infection at 30 DAT ($p < 0.05$). As shown in Table 5, mycorrhizal infection increased from 25.6% in the non-inoculated treatment to 62.2% in the AMF-inoculated treatment, and infection levels stabilized around 60–68% at 50 DAT. Charged biochar also supported higher infection rates (50–68%), indicating a more favorable rhizosphere environment. Root length remained relatively stable (17–19 cm at 30 DAT; 23–26 cm at 50 DAT), showing limited response to treatments. However, root dry weight increased sharply, with 10% AMF producing the highest biomass at 50 DAT (36.9 g hill^{-1}) compared with 20.9 g in the control. Similarly, 5 t ha^{-1} charged biochar improved root biomass (30.6 g hill^{-1}).

3.6. Relationship Between Root Infection and Soil Chemistry, Growth Components, Nutrient Content, and Forage Quality

The ANOVA results showed that the combined application of AMF and charged biochar had significant effects ($p < 0.05$) on rice herbage dry matter, protein yield, and several soil and plant chemical parameters under acidic conditions. Treatments involving both AMF and charged biochar were associated with higher values of these variables than single or control treatments. These results indicate significant treatment-related differences in plant growth and nutrient-related traits, as reflected in increased tillering and forage yield. The application of AMF and charged biochar significantly affected dry biomass, protein yield, silica content, and lignin content ($p < 0.05$), but did not significantly affect rhizosphere soil pH at 50 DAT (Table 6). Silica and lignin contents tended to increase with higher AMF and biochar doses, although this trend was not entirely consistent.

3.7. Relationships among Growth Parameters, Mycorrhizal Colonization, and Plant Chemical Components Based on Pearson Correlation Analysis

According to Pearson's correlation analysis restricted to variables showing significant effects in the ANOVA (Table 7), vegetative growth parameters, including shoot dry weight and plant height, exhibited strong and significant positive correlations with FDW. Silica content also showed a significant positive association with FDW. In contrast, cell wall chemical components (cellulose, hemicellulose, and lignin) did not show significant correlations with growth parameters. Net assimilation rate (NAR) and relative growth rate (RGR) did not show significant correlations with most variables. Photosynthesis- and respiration-related parameters did not show significant correlations with FDW under the experimental conditions.

3.8. Multiple Linear Regression Analysis among Growth Variables, AMF Root Infection, and Chemical Components Affecting Forage Dry Weight (FDW)

The multiple linear regression model was statistically significant ($p < 0.001$), with an R^2 of 0.996, indicating that a large proportion of the variation in FDW was associated with the combined set of predictor variables (Tables 8 & 9). Given the number of predictors relative to sample size, the model was used to describe overall statistical associations rather than to infer individual causal effects.

Nearly all variation in FDW was statistically explained by the studied variables. FDW showed strong positive associations with shoot dry weight, AMF colonization, nitrogen content, and ash content, whereas cell wall components (hemicellulose, cellulose, and lignin) exhibited weaker or indirect statistical associations with FDW. Based on ANOVA results (Table 9) ($F = 175.948$; $p < 0.001$), the multiple regression model involving 16 independent variables simultaneously had a highly significant effect on FDW. The model explained 99.6% of the variation in yield ($R^2 = 0.996$) with a very small prediction error (Std. Error = 0.0326).

The final regression model (Table 10) confirms that increases in shoot dry weight, N content, AMF activity, ash content, and combined fertilizer–ameliorant treatments were the main factors contributing to higher forage dry weight (FDW). Conversely, excessively high plant P content was negatively associated with FDW, which may reflect nutrient imbalance; however, causal mechanisms cannot be inferred from the present analysis.

Table 6. Effect of AMF and charged biochar on dry matter of rice herbage, protein yield, rhizosphere soil pH, Silica and Lignin at 50 days after transplanting (DAT)

Treatment	Dry matter (tons ha^{-1})	protein yield (kg ha^{-1})	Rhizosphere soil pH	Silica (%)	Lignin (%)
AMF application in seedling media (%)					
0.0	1.00±0.13^{b}	90.93 ± 14.31^{b}	5.94±0.05^{a}	2.88 ±0.56^{b}	4.08±0.43^{a}
5.0	1.29±0.99^{ab}	115.63±14.73^{ab}	5.81±0.28^{a}	3.27±0.97^{ab}	3.98±0.57^{ab}
10.0	1.53±0.13^{a}	139.84±16.64^{a}	5.67±0.24^{a}	3.08±0.18^{a}	3.09±0.49^{b}
Charged- biochar (tons ha^{-1})					
0	1.10±0.19^{b}	103.02±14.52^{b}	5.82±0.30^{a}	2.99±0.39^{ab}	3.22±0.46^{b}
2.5	1.25±0.20^{ab}	106.07±24.32^{ab}	5.88±0.16^{a}	2.44±0.51^{b}	4.22±0.41^{a}
5.0	1.48±0.21^{a}	137.32±16.62^{a}	5.72±0.18^{a}	3.79±0.41^{a}	3.73±0.66^{ab}
CV (%)	18.98	19.79	7.09	19.26	13.73

Notes: Mean values in each column marked with different letters indicate statistically significant differences among treatments for AMF or biochar, based on LSD Test at the 5% significance level ($p < 0.05$). Data are presented as mean ± standard deviation. CV = Coefficient of Variation.

Table 7. Pearson correlation matrix among growth parameters, mycorrhizal traits, and plant chemical components

		LAB g m^{-2} day^{-1}	RPR mg g^{-1} day^{-1}	shoot dry weight (g)	plant height (cm)	AMF (%)	FDW (tons ha^{-1})	Silica (%)	Hemi cellulose (%)	Cellulose (%)	Lignin (%)
LAB g m^{-2} day^{-1}	Pearson Correlation	1									
	Sig. (2-tailed)										
RPR mg g^{-1} day^{-1}	Pearson Correlation	.330	1								
	Sig. (2-tailed)	.093									
shoot dry weight (g)	Pearson Correlation	.031	-.104	1							
	Sig. (2-tailed)	.879	.607								
plant height (cm)	Pearson Correlation	-.292	-.283	.637**	1						
	Sig. (2-tailed)	.140	.153	**.000**							
AMF (%)	Pearson Correlation	-.002	-.122	.112	.423*	1					
	Sig. (2-tailed)	.994	.545	.579	**.028**						
FDW (tons ha^{-1})	Pearson Correlation	.040	-.064	.994**	.626**	.107	1				
	Sig. (2-tailed)	.841	.750	**.000**	**.000**	.596					
Silica (%)	Pearson Correlation	.051	.072	.375	.503**	.092	.398*	1			
	Sig. (2-tailed)	.802	.722	.054	.008	.646	**.040**				
Hemi Cellulose (%)	Pearson Correlation	.067	.164	-.069	-.122	-.007	-.067	-.093	1		
	Sig. (2-tailed)	.739	.414	.734	.544	.973	.739	.644			
Cellulose	Pearson Correlation	-.075	-.228	-.101	-.269	-.030	-.121	-.462*	-.510**	1	
	Sig. (2-tailed)	.711	.252	.617	.175	.882	.549	**.015**	**.007**		
Lignin	Pearson Correlation	-.125	.173	-.179	.003	-.014	-.159	.076	-.361	-.111	1
	Sig. (2-tailed)	.535	.389	.371	.989	.945	.429	.705	.064	.583	
	N	27	27	27	27	27	27	27	27	27	27

Remarks: **Correlation is statistically significant at the 0.01 probability level (two-tailed test)
***** Correlation is statistically significant at the 0.05 probability level (two-tailed test).

Table 8. Summary of Multiple Linear Regression Model among Growth Variables, AMF Root Infection, and Chemical Components of the Plant

Model Summary				
Model	R	R Square	Adjusted R Square	Std. Error of the Estimate
1	0.998[a]	0.996	0.991	0.03259

a. Predictors: (Constant), lignin, plant height (cm), N-content (%), P-plant (%), cellulose, ash content (%), root dry weight (g), root length (cm), LAB g m^{-2} day^{-1}, AMF infection in root (%), RPR mg g^{-1} day^{-1}, silica, pH, shoot dry weight (g), hemicellulose, treatment (Charged-biochar and AMF)

Table 9. ANOVA Test Results for the Multiple Linear Regression Model on Forage Dry Weight (FDW)

Model		Sum of Squares	df	Mean Square	F	Sig.
1	Regression	2.991	16	.187	175.948	.000[b]
	Residual	.011	10	.001		
	Total	3.001	26			

a. Dependent Variable: FDW (tons ha^{-1})
b. Predictors: (Constant), lignin, plant height (cm), N-content (%), P-plant (%), cellulose, ash content (%), root dry weight (g), root length (cm), LAB g m^{-2} day^{-1}, AMF infection in root (%), RPR mg g^{-1} day^{-1}, silica, pH, shoot dry weight (g), hemicellulose and treatments.

4. DISCUSSION

Soil analysis revealed that the experimental site was strongly acidic (pH H_2O 4.63), with low alluminium ferrum saturation (7.61%) and iron (Fe) concentration (3616.89 ppm). These conditions indicate a high risk of iron toxicity, which is widely known to inhibit the uptake of essential nutrients such as P, Ca, and Mg, thereby suppressing plant physiological activity and biomass accumulation. The very low availability of these nutrients observed in this study confirms the severity of nutrient stress at the experimental site. Similar conditions have been reported to severely restrict root development and nutrient uptake in acidic soils with pH below 5.5 due to elevated Al and Fe toxicity (Varghese et al., 2022).

Under such adverse soil conditions, improvements in nutrient uptake efficiency and plant physiological performance become critical. The combined application of charged biochar and arbuscular mycorrhizal fungi (AMF) appeared to play a significant role in improving soil–plant functioning. Charged biochar, as a carbon-rich soil amendment, has been reported to ameliorate soil acidity by increasing soil pH and reducing Al and Fe toxicity (Kasno, 2019). In parallel, AMF form symbiotic associations with plant roots, extending the effective root surface area and enhancing the uptake of nutrients, particularly phosphorus, which is often limiting in acidic soils (Paymaneh et al., 2018; Varghese et al., 2022). The integration of these two amendments therefore provides both physicochemical and biological improvements in the rhizosphere, leading to more favorable root-zone conditions and enhanced nutrient availability (Assaye, 2024; Tusar et al., 2025).

The improved soil–plant interactions were reflected in enhanced vegetative growth performance. Pearson correlation analysis showed that shoot dry weight was very strongly and positively correlated with forage dry weight (FDW), indicating that increases in above-ground biomass were closely associated with higher forage productivity. Plant height also exhibited a strong positive correlation with shoot dry weight, suggesting that improved vertical growth contributed to greater biomass accumulation. In addition, AMF colonization was positively correlated with plant height, implying that stronger symbiotic associations supported enhanced vegetative elongation and overall plant vigor.

However, AMF colonization did not show a significant direct correlation with FDW, suggesting that its contribution to yield formation was primarily indirect. Rather than directly increasing forage yield, AMF appeared to support structural growth and biomass development through improved nutrient acquisition and root function. In contrast, physiological indices such as net assimilation rate (NAR) and relative growth rate (RGR) did not show significant correlations with most measured variables, indicating that, under the prevailing experimental conditions, growth variation was driven more by biomass accumulation and canopy development than by changes in intrinsic physiological efficiency.

Silica accumulation emerged as an important supporting factor in plant growth and forage productivity. Silica content showed significant positive correlations with both plant height and FDW, indicating that higher silica accumulation was associated with greater plant sturdiness and biomass yield. Previous studies have demonstrated that silica application enhances plant height, photosynthetic capacity, and biomass production in various crops, including maize and rice (Melo et al., 2024; Prisa, 2023; Yang et al., 2025). Reported silica concentrations in rice typically range from 1.62 to 2.66%, depending on genotype (Gan et al., 2004), and increases in silica content up to an optimal level have been shown to improve net photosynthesis and stress tolerance (Li et al., 2018; Rakian et al., 2023). Nevertheless, excessive silica accumulation may reduce nutrient return under certain conditions, emphasizing the importance of balanced nutrient management.

Table 10. Multiple Linear Regression Coefficients between Growth Variables and Chemical Components on Forage Dry Weight (FDW)

Coefficients[a]

Model		Unstandardized Coefficients		Standardized Coefficients	t	Sig.
		B	Std. Error	Beta		
1	(Constant)	.275	.401		.687	.508
	Treatments (Charged biochar and AMF)	.014	.006	.105	2.446	.034
	LAB g m^{-2} day^{-1}	.004	.017	.007	.256	.803
	RPR mg g^{-1} day^{-1}	.002	.001	.040	1.454	.177
	root dry weight (g)	-.001	.001	-.021	-.601	.561
	ash content (%)	.016	.006	.077	2.484	.032
	shoot dry weight (g)	.101	.004	.982	23.304	.000
	pH	-.049	.024	-.071	-2.037	.069
	root length (cm)	-.005	.003	-.047	-1.831	.097
	plant height (cm)	-.005	.002	-.086	-1.909	.085
	N-content (%)	.173	.063	.077	2.754	.020
	AMF (%)	.001	.001	.077	2.325	.042
	P-plant (%)	-1.303	.580	-.070	-2.246	.048
	Silica (%)	-.009	.012	-.024	-.746	.473
	Hemicellulose (%)	.001	.003	.014	.358	.728
	Cellulose (%)	-.007	.005	-.053	-1.356	.205
	Lignin (%)	.012	.007	.051	1.597	.141

a. Dependent Variable: FDW (tons ha^{-1})

In contrast to silica and vegetative growth parameters, cell wall components exhibited different patterns of association. Cellulose showed a significant negative correlation with both silica and hemicellulose, suggesting a structural trade-off within the cell wall, whereby increases in silica or hemicellulose are accompanied by reductions in the proportional contribution of cellulose. Hemicellulose is known to form strong non-covalent associations with cellulose microfibrils, creating a dense cellulose–hemicellulose matrix (Cosgrove, 2022). Silica further interacts with these components to enhance tissue rigidity and mechanical strength (Singh et al., 2023). Several studies have reported that cellulose content tends to increase under silica-deficient conditions, supporting the inverse relationship observed among these structural components (Huang et al., 2024; Schaller et al., 2022).

Despite these structural interactions, Pearson correlation analysis confirmed that cell wall components (hemicellulose, cellulose, and lignin) were not significantly correlated with FDW. This indicates that while these components are essential for tissue strength, mechanical stability, and stress resilience, they do not directly determine total biomass yield. Previous studies have shown that hemicellulose and lignin contribute to pest resistance, stem stiffness, and lodging resistance, thereby indirectly supporting yield stability rather than directly enhancing biomass accumulation (Hu et al., 2018; Li et al., 2025; Li et al., 2022; Rongpipi et al., 2019).

Multiple regression analysis further clarified the determinants of forage productivity. The regression model showed that FDW was strongly and positively associated with shoot dry weight and nitrogen content, with additional contributions from ash content (reflecting mineral and silica accumulation) and AMF colonization. The very high coefficient of determination (R^2 = 0.996) indicates that most of the variation in FDW was explained by these physiological and nutritional variables. In contrast, phosphorus concentration in plant tissue was negatively associated with FDW, suggesting that excessive P accumulation may lead to nutrient imbalance or antagonistic interactions with other essential elements, such as Zn or Cu. This finding emphasizes that nutrient balance and efficiency are more critical than absolute nutrient concentration under Fe-toxic conditions. Kim and Li (2016) explained that nutrient balance is essential for maximizing growth and yield, as observed in various crops where P levels above a threshold resulted in diminished returns.

The relationships revealed by correlation and regression analyses are closely linked to the underlying soil constraints imposed by Fe toxicity. Variables such as nitrogen status, AMF colonization, silica accumulation, and phosphorus balance are directly influenced by nutrient limitations and chemical stress in acidic soils. The combined application of charged biochar and AMF appears to mitigate these constraints by improving nutrient retention, enhancing root–microbe interactions, and supporting the development of both vegetative biomass and structural tissue components.

Changes in cell wall composition during the early vegetative stage (30–50 DAT) further support this interpretation. While cellulose content remained relatively stable across treatments, hemicellulose content tended to increase under higher AMF inoculation rates, suggesting enhanced cell wall development associated with improved vegetative growth and leaf area expansion. Charged biochar did not significantly affect cellulose content but influenced hemicellulose dynamics, indicating that these amendments primarily affected the more flexible and dynamic components of the cell wall rather than the rigid cellulose framework. Ezquer et al. (2020) demonstrated that higher AMF inoculation rates are associated with increased hemicellulose content, promoting enhanced vegetative growth. Conversely, Clemente-Moreno et al. (2025) confirmed that while hemicellulose dynamics can be beneficial for growth, excessive modification of cell wall components could potentially hinder photosynthetic efficiency and stress tolerance, suggesting a need for balance in cell wall composition management.

In addition, silica content and protein yield of rice herbage increased significantly under AMF inoculation and charged-biochar application, particularly at higher treatment levels. These responses reflect improved nitrogen uptake, enhanced nitrogen-use efficiency, and greater silicon accumulation, which collectively supported stronger vegetative growth. These improvements were largely driven by biological and physicochemical mechanisms rather than direct changes in rhizosphere soil pH, highlighting the importance of integrated soil–plant–microbe interactions.

The observed increases in forage dry weight and shoot biomass confirm that the combined application of AMF and charged biochar effectively enhanced rice vegetative productivity under Fe-toxic conditions. Enhanced root length and root dry weight further explain these responses, as a more developed root system allows more efficient exploration of soil resources. AMF colonization increased the effective absorptive surface area of roots, while charged biochar improved soil chemical conditions and microbial habitat, creating a rhizosphere environment conducive to sustained plant growth. Mulyadi and Jiang (2023) stated that AMF colonization increases the root surface area, allowing more efficient nutrient and water absorption. Furthermore, Li et al. (2023) stated that the presence of biochar also supports microbial habitats, which can further enhance soil fertility and plant health.

Overall, these findings indicate that improvements in rice forage productivity were primarily driven by enhanced vegetative growth, improved nutrient-use efficiency, and silica-mediated structural reinforcement, rather than by direct modification of cell wall composition. While cell wall components contributed to tissue strength, resilience, and forage quality, they played a secondary role in determining total biomass yield. Manonmani et al. (2025) explained that Si contributes to the mechanical strength of rice plants, reducing lodging risks and enhancing resilience against biotic and abiotic stresses. Joy et al. (2025) reported that Si enhances the availability of essential nutrients (N, P, and K) and mitigates nutrient toxicity, which is crucial for rice productivity.

This study was conducted under controlled conditions and focused on early vegetative growth stages. Therefore, future research should examine the persistence of these mechanisms across later growth stages, under field-scale conditions, and in ratoon systems following grain harvest. Given the inherent environmental variability in field conditions and the limited number of sites and seasons evaluated, multi-season and multi-location studies incorporating broader soil biochemical and microbial parameters are recommended to validate and strengthen the applicability of these findings.

5. CONCLUSION

Rice forage productivity under Fe-toxic acidic soil conditions was primarily governed by vegetative growth performance and silica accumulation rather than by direct modification of cell wall components. Strongly acidic soil with high Fe and Al saturation imposed severe nutrient stress; however, the combined application of charged biochar and arbuscular mycorrhizal fungi (AMF) improved soil–plant functioning through enhanced nutrient-use efficiency and plant growth. Forage dry weight was closely associated with shoot dry weight, nitrogen status, ash (silica) content, plant height, and AMF colonization, while cellulose, hemicellulose, and lignin contributed mainly to structural integrity rather than yield formation. AMF promoted biomass production predominantly via improved growth dynamics rather than alteration of cell wall structure. These findings highlight silica accumulation and AMF–charged biochar integration as key mechanisms for mitigating Fe toxicity and enhancing rice forage productivity. Future studies should assess the persistence of these mechanisms across growth stages, particularly under ratoon systems following grain harvest, to support sustainable forage-based rice production on acidic soils.

Acknowledgment

Sincere gratitude is extended to the Ministry of Research, Technology, and Higher Education of the Republic of Indonesia for funding this research through the Fundamental Research Scheme under Contract No. 131/C3/DT.05.00/PL/2025. Appreciation is also extended to the Higher Education Service Institution (LLDIKTI) Region X and the Institute for Research and Community Service (LPPM) of Universitas Tamansiswa Padang for facilitating the implementation of this research.

Declaration of Competing Interest

The authors declare that no competing financial or personal interests may appear to influence the work reported in this paper.

References

Ahmed, S. F., Ullah, H., Aung, M. Z., Tisarum, R., Cha-Um, S., & Datta, A. (2023). Iron Toxicity Tolerance of Rice Genotypes in Relation to Growth, Yield and Physiochemical Characters. *Rice Science*, *30*(4), 321-334. https://doi.org/10.1016/j.rsci.2023.02.002

Akbar, M., Chohan, S. A., Yasin, N. A., Ahmad, A., Akram, W., & Nazir, A. (2023). Mycorrhizal inoculation enhanced tillering in field grown wheat, nutritional enrichment and soil properties. *PeerJ*, *11*, e15686. https://doi.org/10.7717/peerj.15686

Alotaibi, M. O., Ikram, M., Alotaibi, N. M., Hussain, G. S., Ghoneim, A. M., Younis, U., . . . Danish, S. (2023). Examining the role of AMF-Biochar in the regulation of spinach growth attributes, nutrients concentrations, and antioxidant enzymes in mitigating drought stress. *Plant Stress*, *10*, 100205. https://doi.org/10.1016/j.stress.2023.100205

Assaye, Y. M. (2024). Enhancing Rice Seed Production in Ethiopia with Silicon-Rich Biochar. *Research & Development*, *5*(3), 94-96.

Aufa Ain, A. S., & Noraini, M. J. (2023). Effects of rice husk biochar (RHB) with combined inoculation of arbuscular mycorrhizal fungi (AMF) and phosphate solubilizing bacteria (PSB) on growth of maize (Zea mays). *IOP Conference Series: Earth and Environmental Science*, *1131*(1), 012007. https://doi.org/10.1088/1755-1315/1131/1/012007

Clemente-Moreno, M. J., Frey, C., López-Serrano, L., Acebes, J. L., Flexas, J., & Gago, J. (2025). Photosynthesis and stress tolerance: cell walls at the cross-roads. *Journal of Experimental Botany*, *76*(17), 4884-4895. https://doi.org/10.1093/jxb/eraf281

Cosgrove, D. J. (2022). Plant cell growth and cell wall enlargement. *Encyclopedia of Life Sciences (eLS)(Online)*, *2*(11). https://doi.org/10.1002/9780470015902.a0029421

da Silva, K. J. G., Fernandes, J. A. L., Magurno, F., Leandro, L. B. A., Goto, B. T., & Theodoro, R. C. (2022). Phylogenetic Review of Acaulospora (Diversisporales, Glomeromycota) and the Homoplasic Nature of Its Ornamentations. *Journal of Fungi*, *8*(9), 892. https://doi.org/10.3390/jof8090892

de Tombeur, F., Cooke, J., Collard, L., Cisse, D., Saba, F., Lefebvre, D., . . . Cornelis, J.-T. (2021). Biochar affects silicification patterns and physical traits of rice leaves cultivated in a desilicated soil (Ferric Lixisol). *Plant and Soil*, *460*(1), 375-390. https://doi.org/10.1007/s11104-020-04816-6

Du, J., Liu, B., Zhao, T., Xu, X., Lin, H., Ji, Y., . . . Ding, X. (2022). Silica nanoparticles protect rice against biotic and abiotic stresses. *Journal of Nanobiotechnology*, *20*(1), 197. https://doi.org/10.1186/s12951-022-01420-x

Ezquer, I., Salameh, I., Colombo, L., & Kalaitzis, P. (2020). Plant Cell Walls Tackling Climate Change: Biotechnological Strategies to Improve Crop Adaptations and Photosynthesis in Response to Global Warming. *Plants*, *9*(2), 212. https://doi.org/10.3390/plants9020212

Gan, X., Jiang, L., Xu, J., Dong, D., & Wei, S. (2004). Characteristics and genotypic difference of silicon accumulation and distribution in rice. *Plant Nutrition and Fertitizer Science*, *10*(5), 531-535. http://europepmc.org/abstract/CBA/464144 chi

Ghouri, F., Ali, Z., Naeem, M., Ul-Allah, S., Babar, M., Baloch, F. S., . . . Shahid, M. Q. (2022). Effects of Silicon and Selenium in Alleviation of Drought Stress in Rice. *Silicon*, *14*(10), 5453-5461. https://doi.org/10.1007/s12633-021-01277-z

Guo, M., Song, W., & Tian, J. (2020). Biochar-Facilitated Soil Remediation: Mechanisms and Efficacy Variations [Review]. *Frontiers in Environmental Science*, *Volume 8 - 2020*. https://doi.org/10.3389/fenvs.2020.521512

Hailegnaw, N. S., Mercl, F., Pračke, K., Száková, J., & Tlustoš, P. (2019). Mutual relationships of biochar and soil pH, CEC, and exchangeable base cations in a model laboratory experiment. *Journal of Soils and Sediments*, *19*(5), 2405-2416. https://doi.org/10.1007/s11368-019-02264-z

Hu, H., Zhang, R., Tao, Z., Li, X., Li, Y., Huang, J., . . . Peng, L. (2018). Cellulose Synthase Mutants Distinctively Affect Cell Growth and Cell Wall Integrity for Plant Biomass Production in Arabidopsis. *Plant and Cell Physiology*, *59*(6), 1144-1157. https://doi.org/10.1093/pcp/pcy050

Huang, G.-M., Xu, Y.-J., & Wu, Q.-S. (2021). "Mycorrhiza-improved P acquisition of host plants: a mini-review. *GSC Biological and Pharmaceutical Sciences*, *14*(3), 62-67. https://doi.org/10.30574/gscbps.2021.14.3.0063

Huang, S., Pu, L., He, G., Wang, X., Chen, D., Xie, X., . . . Lu, Y. (2024). Silicon in soil and its interaction with nitrogen, phosphorus, and potassium nutrients on rice yield: A case study of paddy fields in the Taihu Lake region, China, without a history of silicon fertilization. *Soil and Tillage Research*, *238*, 106027. https://doi.org/10.1016/j.still.2024.106027

Jabborova, D., Annapurna, K., Azimov, A., Tyagi, S., Pengani, K. R., Sharma, P., . . . Sayyed, R. Z. (2022). Co-inoculation of biochar and arbuscular mycorrhizae for growth promotion and nutrient fortification in soybean under drought conditions [Original Research]. *Frontiers in Plant Science*, *Volume 13 - 2022*. https://doi.org/10.3389/fpls.2022.947547

Jamilah, Rapialdi, & Ernita, M. (2021). Response of soybean (Glycine max L.) that was applied by various liquid organic fertilizer in climate change at acid soil. *IOP Conference Series: Earth and Environmental Science*, *883*(1), 012041. https://doi.org/10.1088/1755-1315/883/1/012041

Joy, M. S., Neetu, S., Rakesh, K., Lalrammawii, C., Nihal, D., Hritik, S., . . . Swati, M. (2025). Impact of silicon fertilization on crop growth, productivity and nutrients enhancement in rice: A review. *Plant Science Today*, *12*(1). https://doi.org/10.14719/pst.4287

Kasno, A. (2019). Perbaikan tanah untuk meningkatkan efektivitas dan efisiensi pemupukan berimbang dan produktivitas lahan kering masam [Improving Soil For Better Fertilization Efficiency and Productivity in Acid Drylands]. *Jurnal Sumberdaya Lahan*, *13*(1), 27-40. https://epublikasi.pertanian.go.id/berkala/jsl/article/view/3346

Khaliq, A., Perveen, S., Alamer, K. H., Zia Ul Haq, M., Rafique, Z., Alsudays, I. M., . . . Attia, H. (2022). Arbuscular Mycorrhizal Fungi Symbiosis to Enhance Plant–Soil Interaction. *Sustainability*, *14*(13), 7840. https://doi.org/10.3390/su14137840

Kim, H.-J., & Li, X. (2016). Effects of Phosphorus on Shoot and Root Growth, Partitioning, and Phosphorus Utilization Efficiency in Lantana. *HortScience*, *51*(8), 1001-1009. https://doi.org/10.21273/hortsci.51.8.1001

Kostryukov, S. G., Matyakubov, H. B., Masterova, Y. Y., Kozlov, A. S., Pryanichnikova, M. K., Pynenkov, A. A., & Khluchina, N. A. (2023). Determination of Lignin, Cellulose, and Hemicellulose in Plant Materials by FTIR Spectroscopy. *Journal of Analytical Chemistry*, *78*(6), 718-727. https://doi.org/10.1134/S1061934823040093

Li, J., Han, Y., Lu, X., Tang, X., Sun, J., Li, M., & Li, L. (2025). Simultaneous regulation of both lignin and cellulose biosynthesis modifies xylem fiber properties in Populus [Original Research]. *Frontiers in Plant Science*, *Volume 16 - 2025*. https://doi.org/10.3389/fpls.2025.1646316

Li, M., Chen, C., Zhang, H., Wang, Z., Song, N., Li, J., . . . Guo, X. (2023). Effects of biochar amendment and organic fertilizer on microbial communities in the rhizosphere soil of wheat in Yellow River Delta saline-alkaline soil [Original Research]. *Frontiers in Microbiology*, *Volume 14 - 2023*. https://doi.org/10.3389/fmicb.2023.1250453 English

Li, Q., Fu, C., Liang, C., Ni, X., Zhao, X., Chen, M., & Ou, L. (2022). Crop Lodging and The Roles of Lignin, Cellulose, and Hemicellulose in Lodging Resistance. *Agronomy*, *12*(8), 1795. https://doi.org/10.3390/agronomy12081795

Li, Z., Song, Z., Yan, Z., Hao, Q., Song, A., Liu, L., . . . Liang, Y. (2018). Silicon enhancement of estimated plant biomass carbon accumulation under abiotic and biotic stresses. A meta-analysis. *Agronomy for Sustainable Development*, *38*(3), 26. https://doi.org/10.1007/s13593-018-0496-4

Magurno, F., Uszok, S., Bierza, K., Bakr, J., Kende, Z., Bessa de Queiroz, M., & Casieri, L. (2024). Glomus mongioiense, a New Species of Arbuscular Mycorrhizal Fungi from Italian Alps and the Phylogeny-Spoiling Issue of Ribosomal Variants in the Glomus Genus. *Agronomy*, *14*(7), 1350. https://doi.org/10.3390/agronomy14071350

Manonmani, M., Rajkumar, K., Ramamoorthy, P., Murugaragavan, R., Jayabalakrishnan, R. M., Jasmine, R., . . . Christy, N. M. P. (2025). Silicon as a key driver of phytolith and phytolith-occluded carbon sequestration for climate change mitigation in rice ecosystems - a review. *Plant Science Today*, *11*(sp4). https://doi.org/10.14719/pst.5815

Melo, M. P., Costa, K. S. d. Q., Oliveira, C. F. d., Lima, H. C. d., Melo, N. C., Moraes, F. K. C., . . . Martins, F. P. (2024). Crescimento e partição da matéria seca de milho submetido a adubação silicatada em solo de Cerrado no Amapá, Brasil. *CONTRIBUCIONES A LAS CIENCIAS SOCIALES*, *17*(4), e5950. https://doi.org/10.55905/revconv.17n.4-044

Meng, L., Cheng, Z., Wang, Y., Li, S., & Clarke, N. (2024). Arbuscular Mycorrhizal Fungal Interacted with Biochar and Enhanced Phosphate-Solubilizing Microorganism Abundance and Phosphorus Uptake in Maize.

Agronomy, *14*(8), 1678. https://doi.org/10.3390/agronomy14081678

Mir, R. A., Bhat, B. A., Yousuf, H., Islam, S. T., Raza, A., Rizvi, M. A., . . . Zargar, S. M. (2022). Multidimensional Role of Silicon to Activate Resilient Plant Growth and to Mitigate Abiotic Stress [Review]. *Frontiers in Plant Science*, *Volume 13 - 2022*. https://doi.org/10.3389/fpls.2022.819658

Mishra, S., Dhada, I., & Haldar, P. (2023). Rice Husk: From Agro-Industrial to Modern Applications. In R. Neelancherry, B. Gao, & A. Wisniewski Jr (Eds.), *Agricultural Waste to Value-Added Products: Technical, Economic and Sustainable Aspects* (pp. 295-320). Springer Nature Singapore. https://doi.org/10.1007/978-981-99-4472-9_14

Mulyadi, & Jiang, L. (2023). The Combined Application of Biochar and Arbuscular Mycorrhizal Fungi (AMF) Enhanced the Physical and Chemical Properties of Soil and Rice Productivity in Indonesia. *Sustainability*, *15*(12), 9782. https://doi.org/10.3390/su15129782

Mundada, P. S., Jadhav, S. V., Salunkhe, S. S., Gurme, S. T., Umdale, S. D., Barmukh, R. B., . . . Ahire, M. L. (2021). Silicon and Plant Responses Under Adverse Environmental Conditions. In A. Husen (Ed.), *Plant Performance Under Environmental Stress : Hormones, Biostimulants and Sustainable Plant Growth Management* (pp. 357-385). Springer International Publishing. https://doi.org/10.1007/978-3-030-78521-5_14

Nawaz, S., Jamil, F., Akhter, P., Hussain, M., Jang, H., & Park, Y.-K. (2023). Valorization of lignocellulosic rice husk producing biosilica and biofuels—a review. *Journal of Physics: Energy*, *5*(1), 012003. https://doi.org/10.1088/2515-7655/aca5b4

Noor, A., Lubis, I., Ghulamahdi, M., Chozin, M. A., Anwar, K., & Wirnas, D. (2012). Pengaruh Konsentrasi Besi dalam Larutan Hara terhadap Gejala Keracunan Besi dan Pertumbuhan Tanaman Padi [The Effect of Iron Concentration in Nutrient Solution to Iron Toxicity Symptoms and Growth of Rice]. *Jurnal Agronomi Indonesia*, *40*(2), 91-98. https://journal.ipb.ac.id/jurnalagronomi/article/download/14311/10646

Olanrewaju, J. S., Sato, K., Yamamoto, S., & Masunaga, T. (2024). Influence of Rice Husk Biochar and Its Application Methods on Silicon Dynamics and Rice Yield in Sandy-Loam Soil. *Applied and Environmental Soil Science*, *2024*(1), 6697604. https://doi.org/10.1155/2024/6697604

Paymaneh, Z., Gryndler, M., Konvalinková, T., Benada, O., Borovička, J., Bukovská, P., . . . Jansa, J. (2018). Soil Matrix Determines the Outcome of Interaction Between Mycorrhizal Symbiosis and Biochar for Andropogon gerardii Growth and Nutrition [Original Research]. *Frontiers in Microbiology*, *Volume 9 - 2018*. https://doi.org/10.3389/fmicb.2018.02862

Pouangam Ngalani, G., Ondo, J. A., Njimou, J. R., Nanseu Njiki, C. P., Prudent, P., & Ngameni, E. (2023). Effect of coffee husk and cocoa pods biochar on phosphorus fixation and release processes in acid soils from West Cameroon. *Soil Use and Management*, *39*(2), 817-832. https://doi.org/10.1111/sum.12894

Prisa, D. (2023). Increasing plant resistance with silicon applications. *World Journal of Advanced Research and Reviews*, *17*(03), 602-608. https://doi.org/10.30574/wjarr.2023.17.3.0413

Rakian, T. C., KILOWASID, H., MUHAMMAD, L., AFA, L. O., RISKYANA, A., Wijayanti, Y., . . . Alam, S. (2023). Soil biological quality in rhizosphere, growth, and yield of upland rice grown on acid soil after amended biochar enriched sap of Kappaphycus alvarezii. *Biodiversitas: Journal of Biological Diversity*, *24*(12), 6780. https://doi.org/10.13057/biodiv/d241241

Ramírez-Olvera, S. M., Trejo-Téllez, L. I., Gómez-Merino, F. C., Ruíz-Posadas, L. d. M., Alcántar-González, E. G., & Saucedo-Veloz, C. (2021). Silicon Stimulates Plant Growth and Metabolism in Rice Plants under Conventional and Osmotic Stress Conditions. *Plants*, *10*(4), 777. https://doi.org/10.3390/plants10040777

Ribeiro, B. S. M. R., Silva, M. R. d., Richter, G. L., Ribas, G. G., Streck, N. A., & Zanon, A. J. (2019). Can leaf area in rice be defined by a mathematical model? *Revista Ceres*, *66*. https://doi.org/10.1590/0034-737X201966030005

Rongpipi, S., Ye, D., Gomez, E. D., & Gomez, E. W. (2019). Progress and Opportunities in the Characterization of Cellulose – An Important Regulator of Cell Wall Growth and Mechanics [Review]. *Frontiers in Plant Science*, *Volume 9 - 2018*. https://doi.org/10.3389/fpls.2018.01894 English

Saikanth, D. R. K., Singh, B. V., Rai, A. K., Kumar, U. S., Surender, Yadav, B., & Singh, O. (2023). Biochar Implementation in Rice Paddies for Addressing Greenhouse Gas Emissions and Nutrient Loss: A Review. *International Journal of Plant & Soil Science*, *35*(18), 610-623. https://doi.org/10.9734/ijpss/2023/v35i183326

Schaller, J., Heimes, R., Ma, J. F., Meunier, J.-D., Shao, J. F., Fujii-Kashino, M., & Knorr, K. H. (2019). Silicon accumulation in rice plant aboveground biomass affects leaf carbon quality. *Plant and Soil*, *444*(1), 399-407. https://doi.org/10.1007/s11104-019-04267-8

Schaller, J., Wu, B., Amelung, W., Hu, Z., Stein, M., Lehndorff, E., & Obst, M. (2022). Silicon as a potential limiting factor for phosphorus availability in paddy soils. *Scientific Reports*, *12*(1), 16329. https://doi.org/10.1038/s41598-022-20805-4

Selvarajh, G., Ch'ng, H. Y., Md Zain, N., Seong Wei, L., Liew, J. Y., Mohammad Azmin, S. N. H., . . . Damrongrak, I. (2024). Enriched rice husk biochar superior to commercial biochar in ameliorating ammonia loss from urea fertilizer and improving plant uptake. *Heliyon*, *10*(11). https://doi.org/10.1016/j.heliyon.2024.e32080

Shifa, S., Worku, M., & Beyene, A. (2025). Compost and biochar application to acidic soils in a hot submoist tropical environment improves the forage yield and quality of Desho grass (Pennisetum pedicellatum Trin.). *All Life*, *18*(1), 2448173. https://doi.org/10.1080/26895293.2024.2448173

Singh, P., Kumar, V., & Sharma, A. (2023). Interaction of silicon with cell wall components in plants: a review. *Journal of Applied and Natural Science*, *15*(2). https://doi.org/10.31018/jans.v15i2.4352

Sun, J., Jia, Q., Li, Y., Zhang, T., Chen, J., Ren, Y., . . . Fu, S. (2022). Effects of Arbuscular Mycorrhizal Fungi and Biochar on Growth, Nutrient Absorption, and Physiological Properties of Maize (Zea mays L.). *Journal of Fungi*, *8*(12), 1275. https://doi.org/10.3390/jof8121275

Tripathi, D., Alonso-Perez, M., & Tiwari, D. K. (2018). Rapid Diagnosis of Soil Nutrients Using Microscopic Techniques. *Microscopy and Microanalysis*, *24*(S1), 680-681. https://doi.org/10.1017/s1431927618003896

Tusar, H. M., Uddin, M. K., Mia, S., Kasim, S., Abd. Wahid, S. B., Makino, T., & Solaiman, Z. (2025). Oxidized alkaline biochar and phosphate solubilizing bacteria mixture enhances direct seeded maize yield in an acid soil [Acidic soil; Maize; Microbes; Phosphorus; Pyrogenic carbon]. *Sains Tanah Journal of Soil Science and Agroclimatology*, *21*(2), 19. https://doi.org/10.20961/stjssa.v21i2.93130

Varghese, E. M., Kour, B., Ramya, S., Kumar, N. S., Jisha, M. S., & Ramakrishnan, B. (2022). Chapter 25 - Rhizosphere microbe-mediated alleviation of aluminum and iron toxicity in acidic soils. In R. C. Dubey & P. Kumar (Eds.), *Rhizosphere Engineering* (pp. 499-526). Academic Press. https://doi.org/10.1016/B978-0-323-89973-4.00003-X

Wen, Y., Wu, R., Qi, D., Xu, T., Chang, W., Li, K., . . . Song, F. (2024). The effect of AMF combined with biochar on plant growth and soil quality under saline-alkali stress: Insights from microbial community analysis. *Ecotoxicology and Environmental Safety*, *281*, 116592. https://doi.org/10.1016/j.ecoenv.2024.116592

Wen, Z., Chen, Y., Liu, Z., & Meng, J. (2022). Biochar and arbuscular mycorrhizal fungi stimulate rice root growth strategy and soil nutrient availability. *European Journal of Soil Biology*, *113*, 103448. https://doi.org/10.1016/j.ejsobi.2022.103448

Yang, Y., Huang, L., Yu, L., Zhu, F., Chang, J., Li, M., . . . Zhan, H. (2025). Silicon Accumulation and Photosynthetic Capacity of Dendrocalamus brandisii in Response to Sodium Silicate Foliar Application Across Vegetative Phenological Stages. *Plants*, *14*(17), 2624. https://doi.org/10.3390/plants14172624

Yao, D., Wu, J., Gao, H., Wu, D., & Wei, Z. (2022). Changes in soil silicon forms and availability as affected by rice straw and its biochar. *European Journal of Soil Science*, *73*(6), e13316. https://doi.org/10.1111/ejss.13316